EAST EUROPEAN JOURNAL OF PHYSICS. **2.** 313-319 (2025)
DOI:10.26565/2312-4334-2025-2-38 ISSN 2312-4334

A NEW APPROACH OF OBTAINING SODIUM METASILICATE FROM DEALUMINATED KAOLIN FOR THE SYNTHESIS OF AMORPHOUS SILICON DIOXIDE NANOPARTICLES

D.B. Puzer, A.C.K. Amuzu, A. Abandoh, I. Nkrumah*, B. Kwakye-Awuah, F.K. Ampong, R.K. Nkum, F. Boakye
Department of Physics, Kwame Nkrumah University of Science and Technology, Kumasi, Ghana
**Corresponding Author email: inkrumah.sci@knust.edu.gh*
Received December 24, 2024; revised March 20, 2025; accepted April 3, 2025

Silicon Dioxide nanoparticles of high purity were synthesized using a novel technique of obtaining sodium metasilicate from dealuminated metakaolin. The process involved taking the dealuminated metakaolin through several recrystallization steps to form sodium metasilicate. This was then converted into silicon dioxide nanoparticles using the sol-gel technique. The nanoparticles were studied by X-ray diffraction, scanning electron microscopy, energy dispersive X-ray analysis, thermogravimetric analysis, Fourier transform infrared spectroscopy and UV-visible optical absorption spectroscopy. The results from all the characterization techniques confirmed that the synthesized product was amorphous silicon dioxide nanoparticles with a high level of purity. This study gives an alternate pathway for obtaining sodium metasilicate from dealuminated metakaolin to synthesize amorphous silicon dioxide nanoparticles for industrial applications.
Keywords: *Amorphous silica; Sol-gel synthesis; Nanoparticles; Characterization; Metakaolin; Sodium metasilicate*
PACS: 61.43.Dq, 81.15.-z, 68.55.-a, 81.07.-b

INTRODUCTION

Silicon dioxide (SiO_2) can be found in nature in both crystalline and amorphous forms. Silica in its crystalline form occurs naturally in three polymorphic phases namely tridymite, quartz, and cristobalite [1-2]. Silica is the primary component of sand and the second most abundant mineral compound on the earth crust [3-4]. Several research works have proven interesting properties associated with nano silica, from their high porosity, thermal stability, tunable size, low toxicity to their higher specific surface area (500-700 m^2/g) [3, 5]. The economic importance of silica nanoparticles is evidenced by its widespread inclusion in various industrial applications such as anti-reflection coatings, photovoltaics, thermal energy storage, sensors, piezoelectric devices, photocatalysis and mixture of concrete [6-9]. As a result of these applications, amorphous silica has been projected to hold a significant share in silica production and is expected to increase in 2022–2030, due to its rising demand from the aforementioned industries [7, 10].

A cursory review of available literature shows that there are several techniques available for the synthesis of silicon dioxide (SiO_2) nanoparticles for a range of industrial applications [11-12]. These include, hydrothermal processes [13], vapor-phase reactions [14] chemical precipitation [15], hydrolysis and condensation reactions [16] and the sol-gel process [17-18]. The conventional industrial method involves a fusing reaction between soda ash and quartz at high temperatures (1700 to 2000 °C) for sodium silicate production, which is then precipitated with sulfuric acid to recover silicon dioxide. This process releases a large amount of greenhouse gases into the atmosphere, notably carbon dioxide contributing to greenhouse gas emissions [19]. It is evident that the conventional processes are environmentally unsustainable and energy-intensive [20-21].

Precursors employed for the production of silicon dioxide may either be synthetic silica from inorganic alkaline silicates or organic silicates such as tetramethyl orthosilicate (TMOS) and tetraethyl orthosilicate (TEOS) [4, 22]. However, these precursors are neither cost-effective nor ecologically friendly due to their high cost and toxicity [23]. Consequently, scholars are currently investigating substitute green precursor sources for synthetic silicon dioxide due to the environmental issues and substantial energy usage linked with these techniques [24-25]. Many researchers have produced silica synthetically using green precursors such as biomass including rice husk, sugarcane bagasse, palm kernel shell, sorghum bagasse, maize leaves and bamboo leaves [18, 26-29].

Meanwhile, the use of inorganic materials like kaolinite clay as a raw material to make sodium silicate as silica precursor has, rarely been reported in literature [24, 25]. Kaolin is an aluminosilicate soft powder clayed mineral containing mainly kaolinite with some trace minerals and impurities. Kaolin, when taken through a dehydroxylation reaction at temperatures between 650 – 800ºC results in formation of amorphous product known as metakaolin [30] . When the metakaolin is completely dealuminated, the resultant residue contains > 95 % amorphous silica and quartz with relatively low impurities of metal oxides [31-32]. Sodium silicate solution (SSS) obtained from metakaolin offers typical advantages including refined and uniform particle size along with the high concentration of silica nanoparticles [33]. In our view, this makes it a likely starting material for the production of synthetic silica.

Cite as: D.B. Puzer, A.C.K. Amuzu, A. Abandoh, I. Nkrumah, B. Kwakye-Awuah, F.K. Ampong, R.K. Nkum, F. Boakye, East Eur. J. Phys. 2, 313 (2025), https://doi.org/10.26565/2312-4334-2025-2-38

Hence this research work examines for the first time the synthesis of amorphous silica nanoparticles (AS – NPs) from de-aluminated metakaolin which is converted into sodium metasilicate and taken through a multi-step recrystallization process before acid hydrolysis and precipitation. The precipitated silica is then further purified through hydrothermal acid purification into amorphous silicon dioxide.

MATERIALS AND METHODS

Materials

Kaolin was obtained from the Ghana Bauxite Company located at Awaso in the western north part of Ghana. Sodium hydroxide (NaOH) pellets (99 wt% purity) and ethanol (98 wt%) were purchased from Analar Normapur, UK, whilst Sulphuric acid (H_2SO_4 95 wt%) and Hydrochloric acid (HCl, 35 wt% and Whatman filter paper (No 1) were purchased from Sigma-Aldrich, Germany. Deionized water (WES laboratory, KNUST) served as solvent and used in the solution preparations. Without additional purification, all of the reagents were employed in their original form.

Methods

Preparation of de-aluminated Metakaolin

The metakaolin was obtained by thermal treatment of kaolinite clay. First, the kaolin clay was physically beneficiated using water to remove unwanted particles including quartz, then decanted and centrifuged to further remove residual quartz particles, dried and calcined at 850 ℃ for 60 minutes to obtain a more reactive phase of kaolin known as metakaolin; which was then leached using 2 M HCl at 105 ^oC for 2 hours to obtain de-aluminated metakaolin.

Preparation of Sodium Metasilicate

Sodium metasilicate solution was prepared by weighing 133.14 g of NaOH and adding it to 100.00 g of dealuminated metakaolin in a 1-litre Teflon beaker and mixed thoroughly. 500 g of H_2O was then gently added to the mixture which results in a spontaneous exothermic reaction thereby causing up to 80 % dissolution of the dealuminated metakaolin. The resultant solution was boiled for a while and then gradually cooled down and subsequently transferred into a Teflon bottle placed in an electric oven at 150 ^oC for approximately 90 minutes to allow for the reaction to complete. The reaction product was recovered at the end of the predetermined time, filtered to separate any unreacted residue from the sodium silicate solution. The sodium silicate solution was kept under normal ambient conditions for 24 hours to crystallize into sodium metasilicate after which it was recovered and filtered to separate it from the mother liquor. The chemical reactions occurring in the synthesis process is stated in Equation 1.

$$SiO_{2(s)} + 2NaOH_{(aq)} \rightarrow Na_aSiO_{3(s)} + H_2O_{(l)} \quad (1)$$

Conversion of Sodium Metasilicate to Sodium silicate solution

After the recrystallization process, the sodium metasilicate was then converted to precipitated silica via acid base neutralization and precipitation reactions. This was done by preparing 2 M of H_2SO_4 solution and used to neutralize and precipitate silica from an aliquot of a solution of the crystallized sodium metasilicate in a 1000 ml borosilicate glass beaker. The whole process was done under continuous stirring using a magnetic stirrer at 120 rpm at ambient temperature. The acid was added dropwise while the stirring continued and the pH of the mixture monitored until the pH reached a neutral point where a white precipitate of silica was obtained and at this point the temperature of the mixture reached 95^oC, the stirring was then halted and the beaker covered to allow the mixture of the precipitate and the mother liquor to cool to near ambient temperature.

Obtaining Silicon Dioxide from Sodium Silicate Solution

The precipitated silica was recovered by filtration, washed with aqueous ethanol solution then copiously with distilled water. The sample was subsequently dried at 105 ^oC in an electric oven overnight; recovered, then ground into fine powder using agate mortar and pestle and then stored in zip lock bag for characterizations. The chemical reactions occurring in the synthesis process is stated in Equations 2.

$$Na_2SiO_{3(s)} + H_2SO_{4(aq)} \rightarrow SiO_{2(s)} + Na_2SO_{4(aq)} + H_2O_{(l)} \quad (2)$$

RESULTS AND DISCUSSION

Chemical composition of De-aluminated metakaolin and as-prepared Sodium silicate

The chemical composition of the de-aluminated kaolin has shown clearly that, it is a suitable precursor for the synthesis of silica due to the fact that it contains over 93 % silicon oxides which readily solubilized in caustic soda solution at relatively low temperature. The precursor according to the XRF analysis contains some impurities of metallic oxides with some significant weight percent as shown in Table 1.

The chemical compositions of the sodium metasilicate obtained from the de-aluminated metakaolin is also shown in Table 1. The data in Table 1 shows that sodium metasilicate contains silicon and sodium oxides as the major chemical

constituents and impurities of metallic oxides derived from the de-aluminated metakaolin. It further shows that the yield of Na_2SiO_3 contained high concentrations of silicon dioxide (63 %) which makes it a good precursor for the synthesis of high purity silica nanoparticles. The recrystallized Na_2SiO_3 inherently exhibited impurities such as oxides of sodium, calcium, aluminum and iron which are characteristics of its precursor, and obviously emanated from the de-aluminated kaolin. The level of purity observed in the sodium silicate obtained in this study are much higher than those obtained in works by [34,16, 35, 36] who synthesised sodium silicate from quartz sand.

Table 1. XRF analysis showing the oxides present in De-aluminated metakaolin and Sodium metasilicate hydrate with their percentage weights

SAMPLES	Oxides/(wt%)				
	SiO_2	Na_2O	CaO	Fe_2O_3	Others
DE-ALMTK	93.573	0.854	0.112	0.235	5.226
S-SLCT	63.000	35.300	0.235	0.198	1.267

DE-ALMTK – De-aluminate metakaolin, S – SLCT – Sodium metasilicate

Structural characteristics of AS – NPs

The structure of the synthesised product was studied by Powder X-Ray Diffraction measurements using a Shimadzu XRD-6000 diffractometer, with Cu-Kα radiation (λ = 0.15408 nm), The equipment was operated at 40 mA and 45 kV for phase analysis using the Bragg-Brentano geometry in the 2θ range 10 to 70 °, scan step of 0.05°. The X-ray diffraction pattern of amorphous silicon dioxide nano particles synthesised from kaolin-based metasilicate is illustrated in Figure 1.

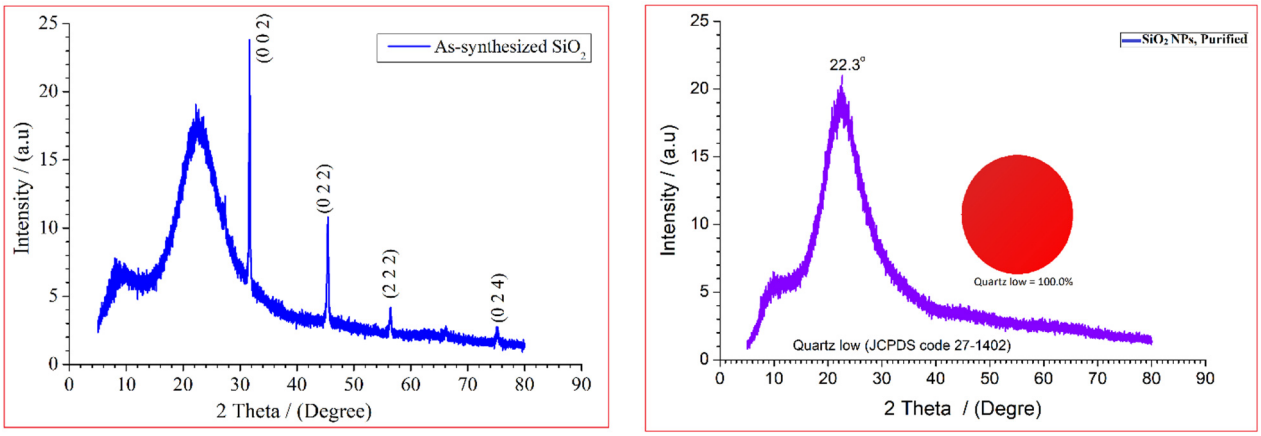

a **b**

Figure 1. XRD patterns of amorphous SiO_2 nanoparticles (a) as-synthesised (b) purified

The XRD pattern of the as-synthesised and purified silicon dioxide nanoparticles are shown in Figures 1a and 1b. The pattern in Figure 1a shows a broad peak in the 2Θ from $22.3\,°\ to\ 28.0°$ which is distinctive of amorphous solid, confirms the formation of amorphous silica [26, 37]. This observation is also in direct accordance with JCPDS 47–0715. The pattern of prominent peaks at positions 31.667, 45.412, 56.404 and 75.175° are indexed to reflections from the (002), (022), (222) and (024) planes of NaCl halite structure (Ref. COD 9008678), which is present as a contaminant. These peaks disappear completely after repeated washings as shown in Figure 1b, leaving behind what appears to be a pure phase of amorphous silicon dioxide. Figure 1b shows a pure phase of amorphous silica with no discernable peaks indexed to impurities.

Morphological and compositional analysis of amorphous SiO_2 nanoparticles

The morphology and elemental composition of synthesised product was studied using a Phenom Pro Desktop FEI Quanta FEG 200 High Resolution Scanning Electron Microscope, integrated with EDS.

SEM and EDX analysis

The micrograph from the SEM analysis of the as-synthesised silicon dioxide is displayed in Figure 2(d) and the corresponding EDS spectrum is depicted in 2(c). As exhibited in Figure 2, it is evident that the morphology shows that, sample consists of a rough surface composed of agglomerates of extremely tiny particles which exhibit irregular shapes and sizes with angular and sharp edges. The EDX spectrum presented in Figure 2 (c) shows that the silicon dioxide contains silicon at 40.63 % and oxygen at 59.37 % with traces of Na, Cl and C elements as impurities for the as-synthesised silica, while Figure 2(b) confirms the purity of the purified silica as it reveals the presence of only Si and O elements having significant intensities. This supports the observations made in the XRD analysis.

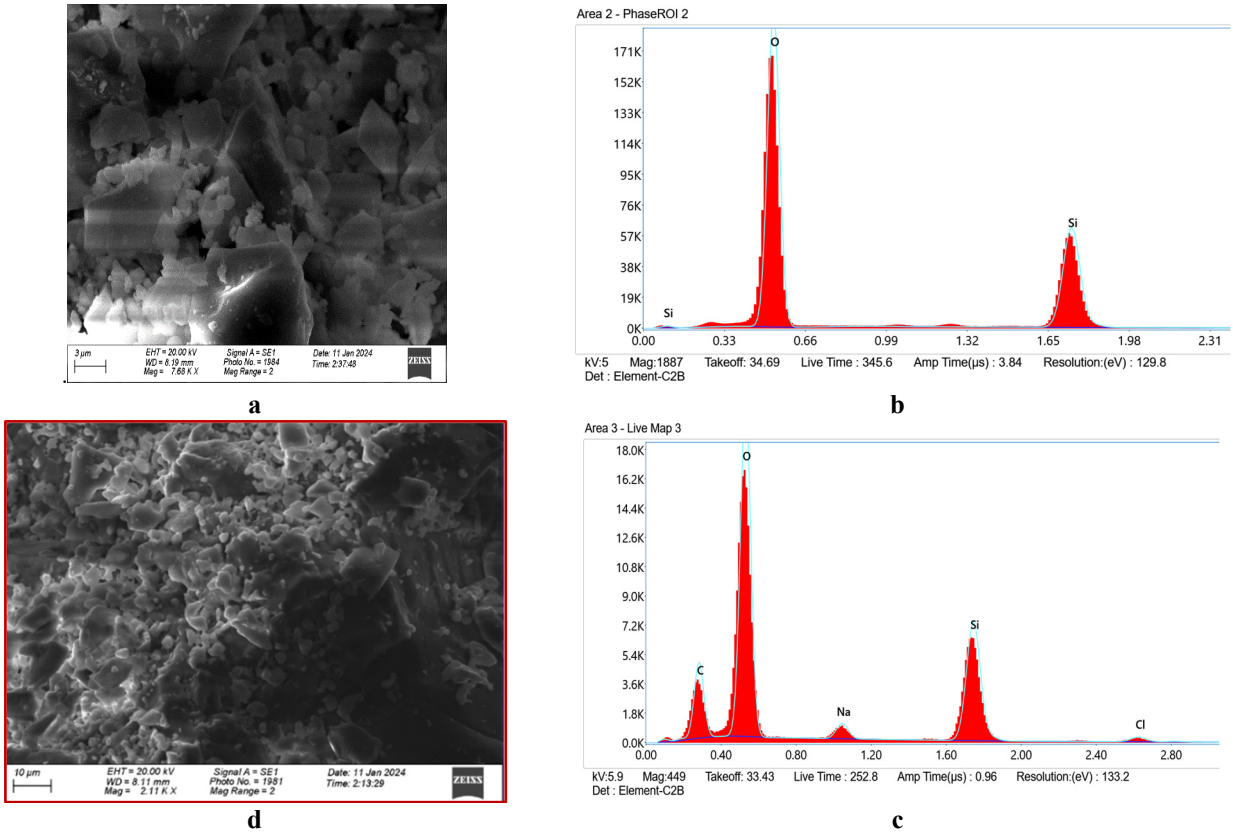

Figure 2. SEM micrograph (d and a) and EDS spectrum (c and b) of the as-synthesised silica and as-purified silica respectively

Thermal Analysis of the synthesised amorphous SiO_2 nanoparticles

To evaluate the thermal stability and phase transition temperature of the prepared SiO_2 nanoparticles, a thermogravimetric study (TGA) was conducted with a TA instrument (SDT Q600 V20.9 Build 20), under the following experimental conditions: temperature ranging from 25 to 1200 ℃; speed of heating 10 ℃/min; sample mass 4.0 mg; under an argon environment; material carrier – ceramic pot. The TGA profile of as-synthesised SiO_2 nanoparticles are depicted in Figure 3.

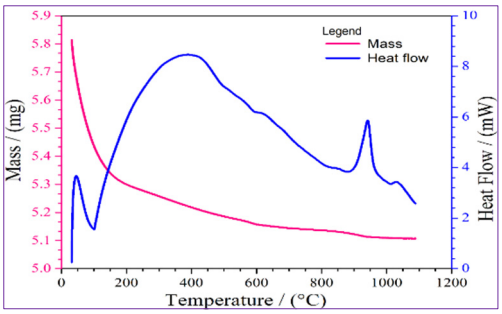

Figure 3. TG/DTA curves of the synthesised pure amorphous silicon dioxide nanoparticles

The thermogravimetric analysis conducted in a temperature range of 25 – 1200 ºC, produced two curves that showed mass lost (in pink) and heat flow (in blue) over time as functions of temperature. The noticeable mass loss from 30 – 150 ºC may be attributable to the evaporation of the absorbed moisture including water of crystallization which gets evaporated and volatile organic compounds present on the surface of the produced nano-silicon dioxide [38]. This initial mass loss indicates the presence of physically absorbed water on the open pore structure and possibly some loosely bound water molecules, which occurs on the silica particle's surface [39]. This suggests quite well that the synthesised silica nanoparticles are stronger absorbers of the surrounding moisture. Some reports have suggested that mass loss due to the presence of physical water is an indication of the porous nature of the material [38, 40]. At temperatures above 1000 °C, the mass loss curve flattens out, indicating no significant further loss in mass. This suggests that all volatile components have been removed, and the remaining material is thermally stable silicon dioxide [34]. Distinct exothermic peaks are also observed at around 800 – 1000 ºC, which may indicate phase transitions or crystallization process within the silicon dioxide nanoparticles. El-didamony et al. (2019) explained that these peaks suggest structural rearrangements that release heat.

Optical analysis of the synthesised amorphous SiO_2 nanoparticles
FTIR Analysis

Fourier transform infrared (FTIR) spectra for the as-synthesised nanoparticles were evaluated via PerkinElmer Spectrum Two photometer (PerkinElmer, USA). The synthesized samples were prepared and placed in a holder constructed of KBr ionic materials and the spectrum is obtained in the wave number range of 400 – 4000 cm^{-1}. A background spectrum was run and subtracted from the compound spectrum. Structural functional group characteristics of the synthesised silica is presented in Figure 4.

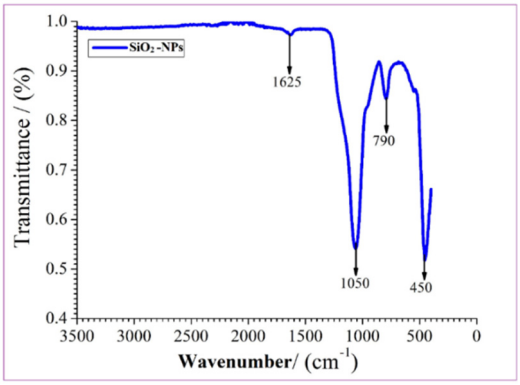

Figure 4. FTIR spectrum of the synthesised silicon dioxide nanoparticles using sodium metasilicate as precursor

The characteristic vibrational functional groups observed in the analyzed spectrum are Si – O – Si, Si – OH and O – Si - O. The synthesized silicon dioxide nanoparticles also exhibited H – O – H groups showing the presence of absorbed molecular water within the sample. The intensities of the peaks in the spectrum characterize the phase purity of the silicon dioxide, thereby corroborating with the EDS data and the XRD results which demonstrated that the silicon dioxide is composed of 100 % quartz low. The asymmetric vibrational mode due to Si – O in the SiO_2 groups occurred at 1050 cm^{-1} while symmetric stretching mode due to Si – Si or Si – O – Si occurred at 790 cm^{-1}. The band at 450 cm^{-1} was due to the bending mode of Si – O – Si or O – Si – O. The observed functional groups in this research are consistent with the reported results in literature [35, 37]. From the FTIR graphs, all peaks relevant to silicon dioxide nanoparticles are observed, thus, further confirming the synthesis of silicon dioxide nanoparticles.

Optical analysis of the synthesised amorphous SiO_2 nanoparticles
UV-Vis absorption spectroscopy

The optical absorption characteristics of the synthesised silicon dioxide nanoparticles at room temperature were studied by UV-Vis spectrophotometer (UV-1800, Shimadzu, Japan). 5.0 mg of each sample was measured into 1:1 ethanol solution to form a colloid. For the measurement of absorbance, the colloid sample was placed in a cuvette with a fixed 1 mm path-length. NaOH solution was utilised as reference to prepare a blank. An illuminated visible light source from the monochromator of constant intensity and low noise over the 200 – 700 nm wavelength range was employed to run through the colloid samples contained in the cuvette.

UV-Vis absorbance spectra of the amorphous SiO_2 were analyzed by plotting $(\alpha h\nu)^2$ as a function of photon energy $(h\nu)$ based on Tauc's relation in the wavelength range of 200 – 700 nm. It can be observed from Figure 5 that the absorbance value was around 385 nm indicating the onset of the fundamental absorption edge.

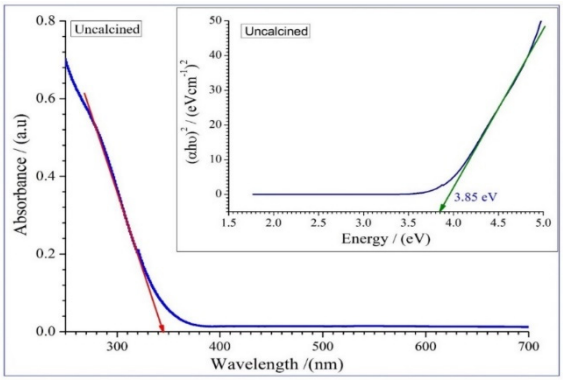

Figure 5. Absorbance spectra of as-synthesized amorphous silicon dioxide nanoparticles.

Figure 5, shows the optical absorbance spectra of the as-synthesised amorphous SiO_2 nanoparticles. It can be observed that the nanoparticles have very low absorbance in the visible range making them almost transparent to visible light. This is an inherent characteristic of amorphous silicon dioxide.

Optical Energy Band Gap (E_g) of the synthesized amorphous SiO_2 nanoparticles

The optical band gap shown inset of Figure 5 is obtained from the absorbance spectra by plotting $(\alpha hv)^2$ against photon energy (hv). The band gap is obtained by drawing a line of best fit, and extrapolating that line to intersect the hv axis where $(\alpha hv)^2$ tends to zero [41]. The point of intersection gives the band gap. From the inset of Figure 5, the energy band gap is 3.85 eV. This high energy band gap is consistent with values reported in previous studies [42, 34]. This observed high band gap energy value shows that the absorption of the silicon dioxide sample is near UV-Vis region, clearly confirming the transparent nature of the synthesised amorphous silicon dioxide nanoparticles.

CONCLUSION

An alternate route for obtaining sodium metasilicate from de-aluminated Kaolin for the synthesis of amorphous silicon dioxide nanoparticles has been established. The physical, structural and thermal characteristics of the synthesized nanoparticles were all authenticated by the XRD, FTIR, SEM, TG/DTA results which were largely congruous with results reported in literature. The findings of the current work show that kaolinite-based clays are prospective alternative precursor for high purity synthesis of amorphous silicon dioxide nanoparticles for potential industrial applications.

Acknowledgements

Authors would like to express their profound gratitude to ZEOTEC Limited Company - Ghana for the provision of instruments and expertise in this research work. We greatly acknowledge the department of Earth Science, University of Ghana, Legon for allowing us to use their TGA machines and RWESCK for their XRD, SEM and EDS characterization tools.

ORCID

D.B. Puzer, https://orcid.org/0009-0001-4470-681X; **A. Abandoh**, https://orcid.org/0009-0004-2465-8277
I. Nkrumah, https://orcid.org/0000-0003-4030-7931; **B. Kwakye-Awuah,** https://orcid.org/0000-0002-8842-681X
F.K. Ampong, https://orcid.org/0000-0003-3562-8183; **R.K. Nkum,** https://orcid.org/0000-0003-0404-760X

References

[1] R.S. Dubey, Y.B.R.D. Rajesh, and M.A. Mor, Materials Today, **2** (4-5), 3575 (2015). https://doi.org/10.1016/j.matpr.2015.07.098
[2] M. Unasir, T. Riwikantoro, M.O.Z. Ainuri, and D. Arminto, Materials Science, **33** (1), 47 (2015). https://doi.org/10.1515/msp-2015-0008
[3] H. Lin, M. Yang, X. Ru, G. Wang, S. Yin, F. Peng, C. Hong, *et al*., Nature Energy, **8**(8), 789 (2023). https://doi.org/10.1038/s41560-023-01255-2
[4] C.P. Faizul, C. Abdullah, and B. Fazlul, Advanced Materials Research, **626,** 997 (2013). https://doi.org/10.4028/www.scientific.net/AMR.626.997
[5] F. Akhter, A. Atta, R. Mahmood, N. Abbasi, S. Ahmed, W. Mukhtiar, and A. Mallah, Silicon, **14** 8295 (2022). https://doi.org/10.1007/s12633-021-01611-5
[6] T. Mizutani, K. Arai, M. Miyamoto, and Y. Kimura, Progress in Organic Coatings, **55**(3), 276 (2006). https://doi.org/10.1016/j.porgcoat.2005.12.001
[7] S.S. Owoeye, S.M. Abegunde, and B. Oji, Nano-Structures & Nano-Objects, **25**, 100625 (2021). https://doi.org/10.1016/j.nanoso.2020.100625
[8] M. Heikal, H. El-didamony, T.M. Sokkary, and I.A. Ahmed, Construction and Building Materials, **38,** 1180 (2013). https://doi.org/10.1016/j.conbuildmat.2012.09.069
[9] N. Meftah, A. Hani, and A. Merdas, Chemistry Africa, **6**(6), 3039 (2023). https://doi.org/10.1007/s42250-023-00688-2
[10] D. Bokov, A.T. Jalil, S. Chupradit, W. Suksatan, M.J. Ansari, I.H. Shewael, G.H. Valley, *et al*., Advances in Materials Science and Engineering, **2021**(1), 5102014 (2021). https://doi.org/10.1155/2021/5102014
[11] F. Farirai, M. Ozonoh, T.C. Aniokete, O. Eterigho-ikelegbe, M. Mupa, and B. Zeyi, International Journal of Sustainable Engineering, **14**(1), 57 (2021). https://doi.org/10.1080/19397038.2020.1720854
[12] V. Zarei, M. Mirzaasadi, A. Davarpanah, A. Nasiri, and M. Valizadeh, Processes, **9**(2), 334 (2021). https://doi.org/doi.org/10.3390/pr9020334
[13] F. Qi, G. Zhu, and Y. Zhang, X. Hou, S. Li, J. Zhang and H. Li, Journal of American Ceramic Society, **104**(1), 535 (2020). https://doi.org/10.1111/jace.17440
[14] P.S. Utama, R. Yamsaengsung, and C. Sangwichien, Brazilian Journal of Chemical Engineering, **36**(1), 523 (2019). https://doi.org/10.1590/0104-6632.20190361s20170458
[15] G.J. Croissant, K.S. Butler, J.I. Zink, and C.J. Brinker, Nature Reviews Materials, **5**(12), 886 (2020). https://doi.org/10.1038/s41578-020-0230-0
[16] Z. Li, D. Wang, F. Lv, J. Chen, C. Wu, Y. Li, J. Shen, and Y. Li, Materials, **15**(3), 970 (2022). https://doi.org/10.3390/ma15030970
[17] S. Rezaei, I. Manoucheri, R. Moradian, and B. Pourabbas, Chemical Engineering Journal, **252,** 11 (2014). https://doi.org/10.1016/j.cej.2014.04.100
[18] U. Zulfiqar, T. Subhani, and S.W. Husain, Journal of Asian Ceramic Societies, **4**(1), 91 (2016). https://doi.org/10.1016/j.jascer.2015.12.001
[19] J. Tao, Cement and Concrete Research, **35**(10), 1943 (2005). https://doi.org/10.1016/j.cemconres.2005.07.004
[20] C.P. Faizul, C. Abdullah, and B. Fazlul, Advanced Materials Research, **626**, 997 (2013). https://doi.org/10.4028/www.scientific.net/AMR.626.997
[21] N.N. Maseko, D. Enke, S.A. Iwarere, O.S. Oluwafemi, and J. Pocock, Sustainability, **15**(5), 4626 (2023). https://doi.org/10.3390/su15054626

[22] G. Zhu, H. Li, X. Wang, S. Li, X. Hou, W. Wu, and Q. Tang, The American Ceramic Society, **99**(8), 2778 (2016). https://doi.org/10.1111/jace.14242
[23] P. Sharma, J. Prakash, R. Kaushal, Environmental Research, **212**, 113328 (2022). https://doi.org/10.1016/j.envres.2022.113328
[24] J.A. Adebisi, J.O. Agunsoye, I.I. Ahmed, S.A. Bello, M. Haris, M.M. Ramakokovhu, and S.B. Hassan, Materials Today: Proceedings, **38**, 669 (2020). https://doi.org/10.1016/j.matpr.2020.03.658
[25] G. Falk, G.P. Shinhe, L.B. Teixeira, E.G. Moraes, and A.P. Navaes de Oliveira, Ceramics International, **45**(17), 21618 (2019). https://doi.org/10.1016/j.ceramint.2019.07.157
[26] P.E. Imoisili, K.O. Ukoba, and T. Jen, Boletín de La Sociedad Española de Cerámica y Vidrio, **59**(4), 159 (2020). https://doi.org/10.1016/j.bsecv.2019.09.006
[27] E. Rafiee, S. Shahebrahimi, M. Feyzi, and M. Shaterzadeh, International Nano Letters, **2**, 29 (2012). https://doi.org/10.1186/2228-5326-2-29
[28] G. Tchanang, C. Njiomou, C. Fon, D. Laure, M. Moukouri, and P. Blanchart, Applied Clay Science, **207**, 106087 (2021). https://doi.org/10.1016/j.clay.2021.106087
[29] V. Vaibhav, U. Vijayalakshmi, and S.M. Roopan, Spectrochimica Acta Part A: Molecular And Biomolecular Spectroscopy, **139,** 515 (2015). https://doi.org/10.1016/j.saa.2014.12.083
[30] B. Kwakye, A. Eric, K. Kyeh, A. Baah, S. Ntiri, I. Nkrumah, and E.V. Kiti, Journal of Thermal Analysis and Calorimetry, **146**, 1991 (2021). https://doi.org/10.1007/s10973-021-10710-9
[31] S.G. Bawa, A.S. Ahmed, and P.C. Okonkwo, Nigerian Journal of Basic And Applied Science, **24**(2), 66 (2016). https://doi.org/10.4314/njbas.v24i2.10
[32] A.B. Eldeeb, V.N. Brichkin, R.V. Kurtenkov, and I.S. Bormotov, Applied Clay Science, **172**, 146 (2018). https://doi.org/10.1016/j.clay.2019.03.008
[33] O. Weichold, B. Tigges, M. Bertmer, and M. Möller, Journal of Colloid and Interface Science, **324**(1-2), 105 (2008). https://doi.org/10.1016/j.jcis.2008.04.060
[34] A. Boualem, L. Leonite, S.A.G. Lopera, and S. Hamzaoui, Silicon, **14**(10), 5231 (2022). https://doi.org/10.1007/s12633-021-01306-x
[35] N. Meftah, A. Hani, and A. Merdas, Chemistry Africa, **6**, 3039 (2023). https://doi.org/10.1007/s42250-023-00688-2
[36] A.B. Prasetyo, I. Agency, M. Handayani, and E. Febrian, Journal of Ceramic Processing Research, **24**(1), 103 (2023). https://doi.org/10.36410/jcpr.2023.24.1.103
[37] N. K. Mohd, N. Nur, A. Nik, and A.A. Azmi, American Institute of Physics, **1885**(1), 020123 (2017). https://doi.org/10.1063/1.5002317
[38] H. El-Didamony, E. El-Fadaly, A.A. Amer, and I.H. Abazeed, Boletín de La Sociedad Española de Cerámica y Vidrio, **9**(1), 31 (2020). https://doi.org/10.1016/j.bsecv.2019.06.004
[39] Q**.** Han, P. Zhang, J. Wu, Y. Jing, D. Zhang, and T. Zhang, Nanotechnology Reviews, **11**(1), 1478 (2022). https://doi.org/10.1515/ntrev-2022-0092
[40] R.K. Kankala, Y. Han, J. Na, C. Lee, Z. Sun, S. Wang, T. Kimura, *et al*., Advanced Materials, **32**(23), 1907035 (2020). https://doi.org/10.1002/adma.201907035
[41] A.Y**.** Oral, E. Mensur, M.H. Aslan, and E. Basaran, Materials Chemistry and Physics, **83**(1), 140 (2004). https://doi.org/10.1016/j.matchemphys.2003.09.015
[42] M.F. Anuar, Y.W. Fen, M.H.M. Zaid, K.A. Matori, and R.E.M. Khaidir, Applied Sciences, **10**(6) 2128 (2020). https://doi.org/10.3390/app10062128

НОВИЙ ПІДХІД ОТРИМАННЯ МЕТАСИЛІКАТУ НАТРІЮ З ДЕАЛЮМІНІСНОВАНОГО КАОЛІНУ ДЛЯ СИНТЕЗУ НАНОЧАСТИНОК АМОРФНОГО ДІОКСИДУ КРЕМНІЮ

Д.Б. Пузер, А.Ч.К. Амузу, А. Абандо, І. Нкрума, Б. Квакі-Авуа, Ф.К. Ампонг, Р.К. Нкум, Ф. Боак'є
Факультет фізики, Університет науки і технологій Кваме Нкрума, Кумасі, Гана

Наночастинки діоксиду кремнію високої чистоти були синтезовані за допомогою нової методики отримання метасилікату натрію з деалюмінованого метакаоліну. Процес передбачав проходження деалюмінованого метакаоліну через кілька етапів перекристалізації з утворенням метасилікату натрію. Потім це було перетворено в наночастинки діоксиду кремнію за допомогою золь-гель техніки. Наночастинки були досліджені за допомогою рентгенівської дифракції, скануючої електронної мікроскопії, енергодисперсійного рентгенівського аналізу, термогравіметричного аналізу, інфрачервоної спектроскопії з перетворенням Фур'є та спектроскопії оптичного поглинання в УФ-видимому діапазоні. Результати всіх методів визначення характеристик підтвердили, що синтезований продукт являв собою аморфні наночастинки діоксиду кремнію з високим рівнем чистоти. Це дослідження пропонує альтернативний шлях отримання метасилікату натрію з деалюмінованого метакаоліну для синтезу наночастинок аморфного діоксиду кремнію для промислового застосування.

Ключові слова: *аморфний кремнезем; золь-гель синтез; наночастинки; характеризація; метакаолін; метасилікат натрію*